THE COMPANY OF
Biologists

RESEARCH ARTICLE

Flagellar adhesion in *Trypanosoma brucei* relies on interactions between different skeletal structures in the flagellum and cell body

Brice Rotureau[1],[*], Thierry Blisnick[1], Ines Subota[1], Daria Julkowska[1], Nadège Cayet[2], Sylvie Perrot[1] and Philippe Bastin[1]

ABSTRACT

The *Trypanosoma brucei* flagellum is an essential organelle anchored along the surface of the cell body through a specialized structure called the flagellum attachment zone (FAZ). Adhesion relies on the interaction of the extracellular portion of two trans-membrane proteins, FLA1 and FLA1BP. Here, we identify FLAM3 as a novel large protein associated with the flagellum skeleton whose ablation inhibits flagellum attachment. FLAM3 does not contain transmembrane domains and its flagellar localization matches closely, but not exactly, that of the paraflagellar rod, an extra-axonemal structure present in the flagellum. Knockdown of FLA1 or FLAM3 triggers similar defects in motility and morphogenesis, characterized by the assembly of a drastically reduced FAZ filament. FLAM3 remains associated with the flagellum skeleton even in the absence of adhesion or a normal paraflagellar rod. However, the protein is dispersed in the cytoplasm when flagellum formation is inhibited. By contrast, FLA1 remains tightly associated with the FAZ filament even in the absence of a flagellum. In these conditions, the extracellular domain of FLA1 points to the cell surface. FLAM3 is essential for proper distribution of FLA1BP, which is restricted to the most proximal portion of the flagellum upon knockdown of FLAM3. We propose that FLAM3 is a key component of the FAZ connectors that link the axoneme to the adhesion zone, hence it acts in an equivalent manner to the FAZ filament complex, but on the side of the flagellum.

KEY WORDS: *Trypanosoma brucei*, Flagellum, Flagellum attachment zone, Paraflagellar rod, FLA1, FLA1BP, FLAM3, Cytoskeleton, Adhesion, Morphogenesis, Division

INTRODUCTION

Trypanosoma brucei is an extracellular protist parasite transmitted by the bite of the tsetse fly. It causes African trypanosomiasis in sub-Saharan Africa, a fatal disease also called sleeping sickness in humans and nagana in cattle (Brun et al., 2010). The parasite cycle is characterized by the existence of multiple developmental stages that can be distinguished according to their general morphology, the type of their surface antigen coat and the distribution of their DNA content (Sharma et al., 2009). All of these forms present a single flagellum, ranging from 3 μm to 30 μm in length, which is attached to the

[1]Trypanosome Cell Biology Unit, Institut Pasteur and CNRS URA 2581, 25 Rue du Docteur Roux, 75015 Paris, France. [2]Plateforme de Microscopie Electronique, Institut Pasteur, 25 Rue du Docteur Roux, 75015 Paris, France.

*Author for correspondence (rotureau@pasteur.fr)

cell body (Rotureau et al., 2011). The flagellum is an essential organelle for trypanosomes because it is involved in motility (Bastin et al., 1998; Branche et al., 2006; Broadhead et al., 2006), cell division (Ralston et al., 2006), morphogenesis (Kohl et al., 2003), attachment to the salivary glands (Tetley and Vickerman, 1985) and infectivity (Griffiths et al., 2007; Emmer et al., 2010).

The trypanosome flagellum is composed of an axoneme (nine microtubule doublets and a central pair) associated with a paraflagellar rod (PFR) and enveloped by the flagellar membrane (reviewed by Vaughan, 2010). The flagellum is nucleated by a basal body physically linked to the condensed genetic material of the single mitochondrion called the kinetoplast (Robinson and Gull, 1991). The flagellum emerges out of the cell body from a specialized membrane invagination known as the flagellar pocket and is attached along the cell body with the exception of its far distal tip. Adhesion of the flagellum to the cell body is mediated by the flagellum attachment zone (FAZ), a kind of 'macula adherens' composed of two sets of structures (Vickerman, 1969). A defined subset follows the exact path of the flagellum inside the cell body and is intercalated within the corset of subpellicular microtubules. It is constituted of an electron-dense pearl-necklace-like filament periodically punctuated by large complexes that are associated with a specialized microtubule quartet (Vickerman, 1969; Sherwin and Gull, 1989a). Different structures are found on the flagellum side, which emerge from doublet 7 of the axoneme to point towards the adhesion region (Vickerman, 1969). These have been termed 'FAZ connectors' (Ralston et al., 2009), but like the FAZ filament, they do not cross membranes (Vickerman, 1969).

Flagellum attachment to the cell body appears vital to trypanosomes (see below) and has been proposed to play at least two essential functions. First, such a specific disposition would facilitate cell movement in a highly viscous or crowded environment (Rodríguez et al., 2009; Weiße et al., 2012). Since the flagellum tip is at the anterior pole of the cell, it could contribute to orientated cell motion and favor transfer of proteins or antibodies bound to the cell surface towards the flagellar pocket situated at the posterior end of the cell (Engstler et al., 2007; Rocha et al., 2010). Second, the FAZ has been proposed to define the axis of cell division and to control the length of the daughter cell (Robinson et al., 1995; Kohl et al., 2003; Zhou et al., 2011). During the cell cycle, assembly of the new FAZ filament initiates early and independently of the flagellum (Kohl et al., 1999; Kohl et al., 2003). Next, its elongation is carried out in parallel to the assembly of the new flagellum (Kohl et al., 2003; Absalon et al., 2007; Zhou et al., 2011). Then, cell division initiates at the anterior extremity of the new FAZ that would act as a cleavage furrow along which cytokinesis progresses posteriorly.

The FAZ filament is an elaborate structure that contains multiple molecular components. Several of them have been

Journal of Cell Science

identified in immunological screens using antibodies from infected patients (reviewed by Kohl and Gull, 1998) or from animals immunized with trypanosome cytoskeletal structures (Woods et al., 1989; Kohl et al., 1999). In *T. brucei*, the DOT-1 antibody stains the FAZ filament, but the antigen it detects has not yet been identified. Nevertheless, the antibody has been used as a reliable marker of the FAZ (Woods et al., 1989). FAZ1 is a large protein (close to 200 kDa) containing multiple repetitions of a unique 14-amino-acid sequence. Its ablation by RNAi does not inhibit the assembly of the filament but perturbs flagellum adhesion and nucleus segregation, further implicating the FAZ filament in cell morphogenesis (Vaughan et al., 2008). Finally, a coiled-coil-rich protein containing a C2-domain (CC2D) was identified in a proteomic screen of skeletal proteins associated with the flagellum (Zhou et al., 2010). Importantly, RNAi knockdown of CC2D blocks the assembly of the FAZ filament without affecting the formation of the four microtubules. This results in complete flagellum detachment and in spectacular morphogenetic defects, leading to the formation of tiny cells whose length is directly correlated to that of the residual FAZ filament (Zhou et al., 2011). These results formally demonstrate the involvement of the FAZ filament in both flagellum attachment and cell morphogenesis.

However, all these proteins are localized within the cell body, raising the question of the mechanism responsible for flagellum adhesion to the cell body. Another family of proteins involved in flagellum attachment comprises transmembrane proteins. The first member was discovered in *Trypanosoma cruzi* as a glycoprotein named GP72, which contains a C-terminal short cytoplasmic sequence, a transmembrane domain and a large extracellular portion that is heavily glycosylated (Cooper et al., 1991). It is conserved in *T. brucei* as a 546 amino acid transmembrane glycoprotein called FLA1 composed of a short intra-cellular C-terminal end (16 aa) and a long N- and O-glycosylated N-terminal extracellular tail (475 aa). In *T. cruzi*, *GP72*-null mutants, albeit viable, exhibit detached flagella and morphological changes characterized by a shorter cell body (Cooper et al., 1993; Rocha et al., 2006). Similarly, silencing of *FLA1* in *T. brucei* leads to flagellum detachment and morphological changes, but also causes cytokinesis defects ultimately resulting in cell death (LaCount et al., 2002). In *T. cruzi*, the phenotype of the $GP72^{-/-}$ cell line could be complemented by the expression of a GP72 protein containing a triple HA tag inserted at the N-terminus, immediately after the signal sequence. Immunostaining revealed a surface location for the tagged protein with a higher concentration on the flagellum and in the flagellar pocket (Haynes et al., 1996; Nozaki et al., 1996). Similarly, an antibody raised against an extracellular portion of the *T. brucei* FLA1 (aa 81–312) localized the protein to the cell surface with a stronger signal on the flagellum (Nozaki et al., 1996). Recently, the differential distributions of truncated versions of FLA1 revealed that its long extracellular N-terminus end interacts with a flagellum partner and that its short C-terminus end is necessary for correct targeting to the FAZ region. However, the exact localization of FLA1 in the FAZ region remains undetermined. In the same study, a transmembrane protein situated on the flagellum side and following the FAZ region was immunoprecipitated with FLA1 (Sun et al., 2012). RNAi silencing of this FLA1-binding protein (FLA1BP) resulted in detached flagella, but curiously had no effect on cell growth in culture (Sun et al., 2012). Parasites expressing truncated versions of FLA1BP without the long extracellular domain also presented

detached flagella, demonstrating the role of the FLA1BP–FLA1 interaction for proper flagellum anchorage along the cell body (Sun et al., 2012). These recent results show that flagellum detachment alone might not be the cause of the cytokinesis defect leading to growth arrest. Therefore, independently of its function in flagellum attachment, the role of FLA1 in cell division remains unclear. Its presence at the flagellar pocket could mediate correct positioning of the flagellum at the cell surface to ensure attachment during flagellum elongation, as well as correct positioning and priming of the FAZ root to ensure a proper orientation and path for cytokinesis.

To address these questions, we investigated a novel large protein associated with the flagellum skeleton, termed FLAM3, whose ablation inhibited flagellum attachment and cell growth. In cells deprived of FLAM3, FLA1 is located in the short FAZ filament but FLA1BP is jammed at the base of the detached flagellum. FLAM3 does not contain transmembrane domains and accesses the flagellum even in the absence of FLA1. Moreover, in cells with reduced or no PFR, both FLA1 and FLAM3 are properly distributed along the FAZ and ensure flagellum attachment. Thus, we propose that FLAM3 is a key component of the FAZ connectors that appear to link the axoneme to the adhesion zone, hence acting in an equivalent manner to the FAZ filament complex, but on the flagellum side. To further understand the mechanism of flagellum adhesion, the precise intracellular localization of FLA1 was also investigated, revealing its association with the FAZ filament through its cytoplasmic tail, independently of flagellum adhesion or presence. A detailed characterization of the phenotype of cells deprived of FLA1 or FLAM3 revealed that the presence of a full-length AND attached flagellum is essential for proper FAZ elongation.

RESULTS

FLA1 localizes to the FAZ filament and is connected to the flagellum skeleton

A recent study in *T. brucei* revealed that the long extracellular N-terminus end of FLA1 is linked to a flagellum membrane partner protein called FLA1BP, and that its short C-terminus end is necessary for correct targeting to the flagellum adhesion region (Sun et al., 2012). However, the precise localization of FLA1 in the FAZ region has not been established so far. Double immunostaining with a rat polyclonal antibody targeting the extracellular portion of FLA1 (Nozaki et al., 1996) and with the mouse monoclonal antibody L3B2, which detects FAZ1 (Kohl et al., 1999; Vaughan et al., 2008) was carried out on procyclic *T. brucei* cells grown in culture. It showed an almost perfect colocalization in intact cells (Fig. 1A). Both signals were resistant to detergent extraction (Fig. 1B), showing that FLA1 is tightly associated with the cytoskeleton. Given the close proximity of the FAZ filament with the four microtubules and the limited resolution of light microscopy, we used two independent biochemical treatments to dissociate these structures. First, the FAZ filament can be depolymerized upon incubation of trypanosome cytoskeletons with 1M NaCl without affecting the four associated microtubules (Sherwin and Gull, 1989b). This resulted in the loss of FAZ1 signal as expected, but also of the FLA1 signal (Fig. 1C), indicating that FLA1 is associated to the FAZ filament. This was confirmed by treatment of cytoskeletons with calcium chloride, which removes the microtubule corset including the four microtubules, but does not affect the FAZ filament (Moreira-Leite et al., 2001). In these conditions, FLA1 still colocalizes with FAZ1 along the FAZ filament (Fig. 1D).
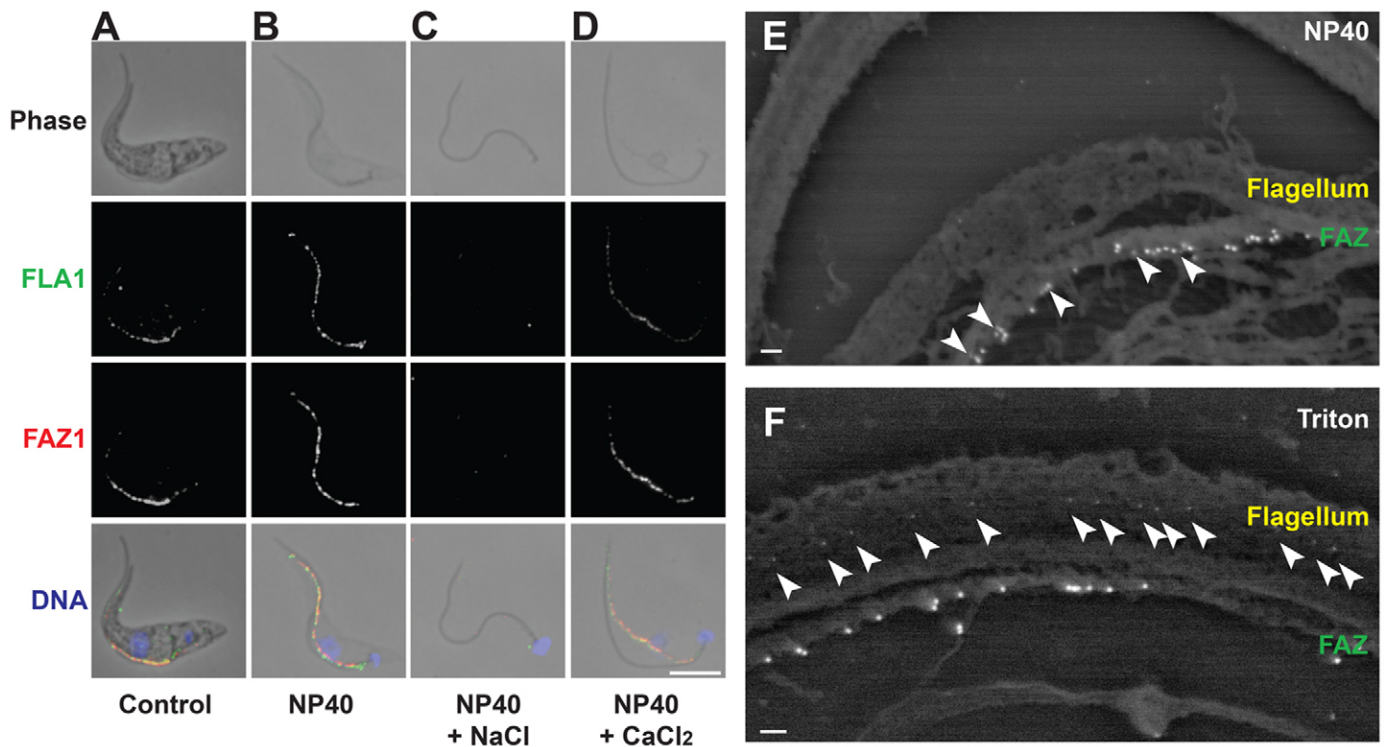
Fig. 1. FLA1 localizes to the FAZ filament. (A–D) Samples were treated as indicated, with or without NP40, NaCl or CaCl$_2$, fixed in methanol and processed for IFA with the anti-FLA1 antibody Flap2 and the anti-FAZ1 antibody L3B2. Scale bar: 5 µm. (E,F) Trypanosomes were treated with NP-40 (E) or Triton X-100 (F), processed for immunogold labeling and observed by scanning electron microscopy. FLA1 (arrowheads indicate 10 nm beads) was observed at the FAZ filament close to FAZ1 (20 nm beads) upon NP-40 treatment, or at the axoneme–PFR junction upon treatment with Triton X-100. Scale bars: 100 nm.

These data are in agreement with a tight association of FLA1 with the FAZ filament but not with the four associated microtubules. Scanning electron microscopy using immunogold staining of detergent-extracted cytoskeletons treated with Nonidet NP-40 further supported this conclusion by showing that FLA1 and FAZ1 colocalized at the same face of the FAZ filament, whereas little or no signal was detected on other structures (Fig. 1E). However, in a small proportion of cells, treatment with the detergent Triton X-100 resulted in a different profile: whereas FAZ1 was still distributed along the FAZ filament, FLA1 was found in the flagellum, as regular spots along a line in the axoneme (Fig. 1F). This suggests the existence of an interaction between FLA1 and the flagellum skeleton. Because FLA1BP is a transmembrane protein (Sun et al., 2012), its intracellular domain could be either directly associated with flagellar structural elements or indirectly associated through other partners.

FLAM3 is a new flagellar protein involved in flagellum anchoring
To identify new flagellum proteins potentially involved in flagellum attachment, we analyzed the composition of trypanosome flagella purified from the $FLA1^{RNAi}$ mutant (unpublished results). Purification was achieved by mechanical shearing, instead of detergent treatment, ensuring the presence of membrane and matrix components in addition to skeletal elements. Several novel proteins were identified and our attention was caught by a protein called flagellum member 3 or FLAM3, encoded by gene Tb927.8.4780. This large 468 kDa protein of 4151 aa contains a TPR-like domain and an antimicrobial defensin-β signal but no predicted transmembrane domain. Orthologous sequences were also found in the genome

of *Trypanosoma brucei gambiense*, *T. congolense*, *T. vivax* and *T. cruzi*, as well as in all *Leishmania* species but not outside the Kinetoplastid group. A FLAM3::YFP fusion protein was expressed upon endogenous tagging in wild-type parasites (Fig. 2). In live cells, the FLAM3::YFP protein was observed in the flagellum, which was confirmed after fixation in paraformaldehyde (Fig. 2A) or methanol (Fig. 2B). FLAM3 was still present at the flagellum after detergent treatment, indicating an association with the flagellum skeleton (Fig. 2C). Double immunofluorescence analysis with an anti-GFP antibody (which also detects YFP) and the FAZ marker L3B2 showed that YFP::FLAM3 distribution was distinct from the FAZ filament, directly following the path of the flagellum and ending more distally (Fig. 2C). However, it did not extend to the flagellum tip, as confirmed by triple immunofluorescence staining with anti-GFP, the anti-axoneme mAb25 and the PFR marker L8C4 (Fig. 2D). At the proximal region of the flagellum, FLAM3::YFP distribution was close to that of the axoneme but distinct from that of the PFR, starting more proximally in the flagellar pocket (see magnification in Fig. 2D). Its initial point appears slightly shifted compared with that of the axoneme labeled by mAb25. Unfortunately, we were not able to detect FLAM3::YFP by scanning electron microscopy after immunogold staining with anti-GFP antibodies.

Nevertheless, such localization is compatible with an involvement in flagellum attachment and was investigated by inducible RNAi silencing in the 29.13 cell line (Wirtz et al., 1999; Wang et al., 2000). The efficiency of the knockdown strategy was verified by RT-PCR with a strong decrease of *FLAM3* mRNA after 48 hours of induction (Fig. 3A). After 24 hours of
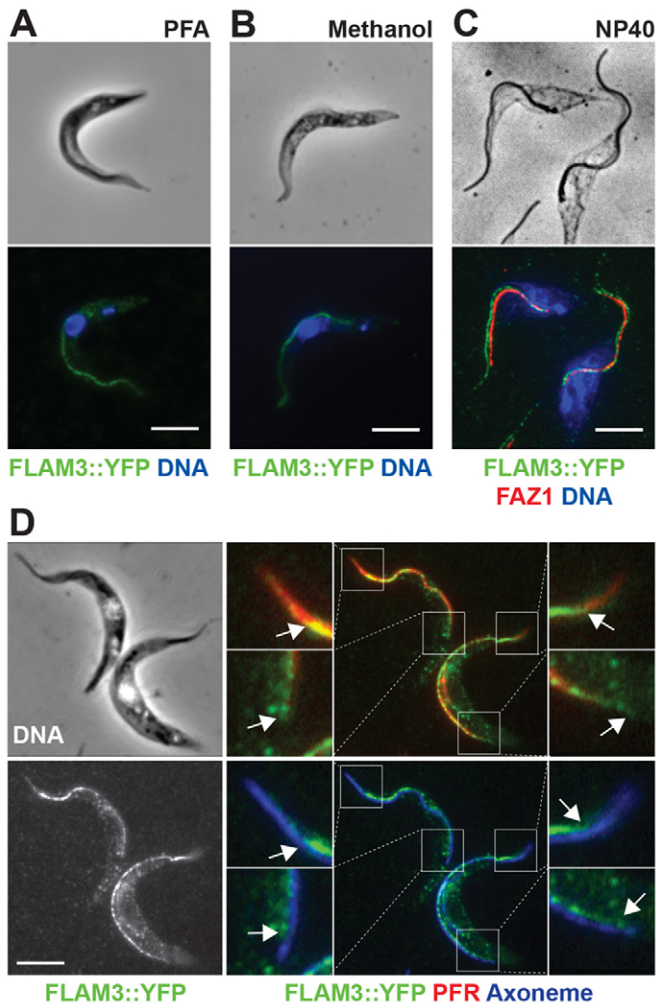
Fig. 2. FLAM3 is a new protein associated with the flagellum skeleton. FLAM3::YFP cells were directly observed after fixation in paraformaldehyde (PFA; A) or treated with methanol (B,D), or first treated with Nonidet P-40 treatment and fixed in methanol (C). Samples were stained with DAPI (blue in A–C or white in D), an anti-GFP (green), the anti-FAZ1 antibody L3B2 (red in C), or the anti-PFR2 antibody L8C4 (red in D) and the axonemal marker Mab25 (blue in D). Immunostaining at the flagellum extremities are detailed in the enlarged boxes (D). Scale bars: 5 µm. Arrows indicate the end of the FLAM3::YFP signal.

induction, cell growth progressively slowed down to definitively stop after two passages (Fig. 3B). Strikingly, microscope examination revealed that after 72 hours of induction, virtually all induced cells presented a detached flagellum (Fig. 3C,D). Analysis by transmission electron microscopy showed that the structural organization of the PFR and of the axoneme looked normal, without visible alteration (supplementary material Fig. S1). Because the FAZ connectors have been proposed to link the PFR to the FAZ region on the flagellum side (Bastin et al., 2000b), we examined flagellum cross-sections of $FLAM3^{RNAi}$ cells to evaluate their presence and organization. Although a fragment of the FAZ connector was apparently absent from detached flagella of most induced cells, a non-ambiguous conclusion could not be reached owing to the difficulty of precisely defining these structures. The $FLAM3^{RNAi}$ phenotype therefore appears very similar to that observed in $FLA1^{RNAi}$ because it results in flagellum detachment without visible modification of flagellum structure.

To compare the two phenotypes, motility, DNA content and morphogenesis were investigated (Fig. 4). Tracking experiments in both $FLA1^{RNAi}$ and $FLAM3^{RNAi}$ mutants revealed that their swimming paths were shortened and their velocity significantly reduced after 72 hours of induction (Fig. 4A,B). In both mutants, the proportion of cells with a detached flagellum increased rapidly during the course of induction (Fig. 4C,D). Analysis of DNA content revealed the emergence of cells with multiple kinetoplasts and nuclei, indicative of cytokinesis defects (Fig. 4C,D). As in other mutants exhibiting flagellum detachment, the length of the FAZ was strongly reduced, as shown by FAZ1 staining (Fig. 4E,H). In both $FLA1^{RNAi}$ and $FLAM3^{RNAi}$ 1K1N cells induced for 72 hours, the distances between the nucleus and the kinetoplast, as well as the distance between the nucleus and the posterior end of the cell remained unchanged compared with that in uninduced control parasites (Fig. 4F,G). Whereas flagellum length, measured by the use of axoneme or PFR markers, was similar in both induced and non-induced conditions (≈ 16 µm), the cell body length and the FAZ length were significantly shorter in induced parasites (Fig. 4F,G). This demonstrates that depletion of FLA1 or FLAM3 and the resulting flagellum detachment do not affect flagellum elongation, but in contrast, drastically limit FAZ elongation. Therefore, to better understand the exact link between FLAM3 and the FAZ structures, we investigated its distribution and compared it with that of FLA1 in various RNAi mutant where flagellum composition or formation is compromised.

Targeting of FLA1 and FLAM3 to the FAZ is independent of flagellum attachment

First, the distribution of FLA1 was examined in two separate mutants exhibiting flagellum detachment. Depletion of KIF9B resulted in severe defects in PFR assembly accompanied by flagellum detachment and formation of a shorter FAZ filament as confirmed by FAZ1 staining (Fig. 5A,B). Nevertheless, FLA1 still localized to the FAZ filament, showing that perturbation of PFR assembly does not interfere with its correct targeting. We then examined distribution of FLA1 in the $PF16^{RNAi}$ mutant where the absence of a central pair protein results in flagellum paralysis, defects in basal body migration, flagellum detachment and formation of a shorter FAZ filament (Absalon et al., 2007). Despite flagellar detachment, FLA1 still localized to the FAZ in $PF16^{RNAi}$ cells (Fig. 5C). This shows that FLA1 targeting to the FAZ filament is independent of flagellum attachment. FLAM3 is present on the flagellum side and its localization matches closely that of the PFR. Thus, we used two distinct mutants to investigate the possible interaction of FLAM3 with the PFR. FLAM3::YFP was still homogeneously distributed along flagella of snl-2 mutants (Fig. 5D,E) that are deprived of PFR2 and fail to assemble most of the PFR (Bastin et al., 2000a). However, a rudimentary PFR is still assembled in these mutants (Bastin et al., 1998). We next investigated FLAM3::YFP distribution in the $KIF9B^{RNAi}$ mutants that exhibit some flagellum regions with only the axoneme and others with massive blocks of PFR material (Demonchy et al., 2009). Here too, FLAM3::YFP localized normally to the axoneme along the entire flagellum (Fig. 5F). Therefore, FLAM3 assembly in the flagellum skeleton appears to be independent of the PFR.

FLA1, but not FLAM3, is properly targeted irrespective of the presence of a flagellum

Inhibition of intraflagellar transport (IFT), the machinery required for flagellum construction is accompanied by the formation of
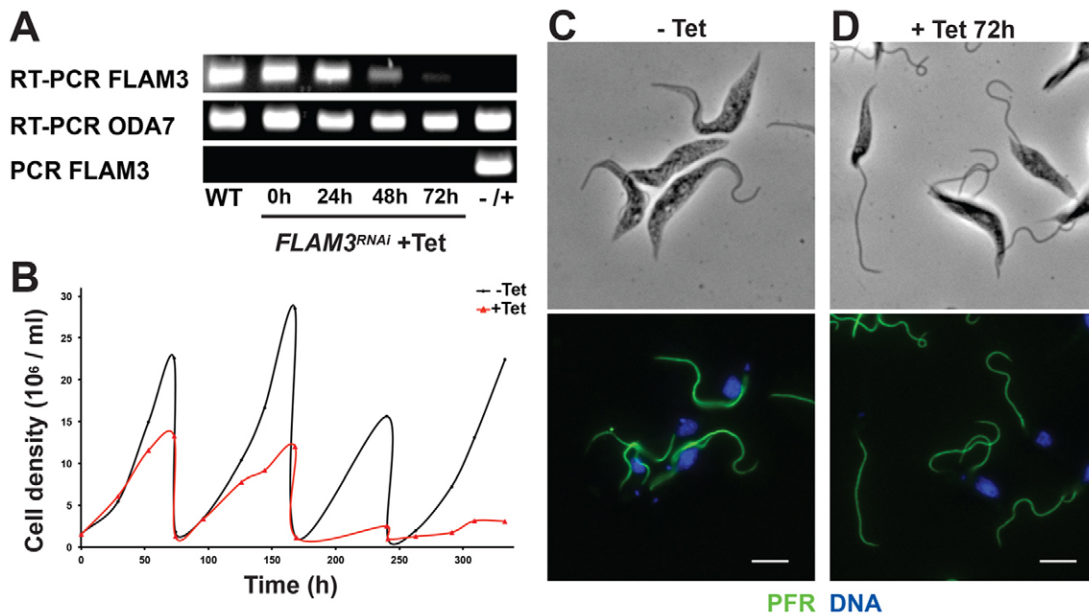
Fig. 3. FLAM3 is involved in flagellum attachment. (A) RT-PCR targeting *FLAM3* mRNA was performed on total RNA extracts from *FLAM3^RNAi* cells at different induction times (0, 24, 48 and 72 hours). RT-PCR targeting *ODA7* mRNA and simple PCR targeting the *FLAM3* DNA coding sequence were carried out on the same samples as positive and negative controls, respectively. Internal negative control with H$_2$O for RT-PCR against *FLAM3*, and positive controls with genomic DNA for RT-PCR against *ODA7* and PCR against *FLAM3* are also shown in the last lane (−/+). Knockdown of *FLAM3* appeared to be effective from 48 hours. (B) Representative growth curves of uninduced (−Tet in black) and induced (+Tet in red) *FLAM3^RNAi* cells. Cell densities are plotted in millions of cells per ml and cells were diluted to 1 million per ml every 72 hours. (C,D) *FLAM3^RNAi* cells uninduced (C) or induced for 72 hours (D) were fixed in methanol and stained with DAPI (blue) and the anti-PFR2 antibody L8C4 (green). Scale bars: 5 µm.

much shorter FAZ structures (Kohl et al., 2003; Absalon et al., 2007). Anterograde IFT is halted in the *IFT88^RNAi* cell line, resulting in the absence of a flagellum (Kohl et al., 2003). Localization of FLAM3::YFP was limited to the cytoplasm in non-flagellated induced *IFT88^RNAi* cells lacking anterograde transport (Fig. 6A) and the whole protein pool was lost upon detergent treatment. By contrast, FLA1 remained associated with the short FAZ and fully merged with FAZ1 (Fig. 6B). These results could be explained either by the loss of IFT or by a failure to form a flagellum. We therefore examined *IFT140^RNAi* parasites that fail in retrograde transport, leading to the assembly of a tiny flagellum accumulating IFT proteins in a bulky extension (Absalon et al., 2008a). FLAM3::YFP was concentrated in the short bulky flagella of *IFT140^RNAi* parasites where retrograde transport was inhibited (Fig. 6C), and the whole protein pool was also lost upon detergent treatment (not shown). This indicates that FLAM3 cannot associate with the remaining FAZ structure in the absence of a flagellum. Thus, FLAM3 is targeted to the flagellum as a skeletal component.

Although inhibition of IFT blocks assembly of flagellar microtubules and associated structures, the flagellum membrane still elongates and appears stuck to the cell surface, forming a so-called 'flagellar sleeve' (Davidge et al., 2006; Absalon et al., 2008b; Adhiambo et al., 2009). To evaluate whether the extracellular domain of FLA1 was still present at the surface in *IFT140^RNAi* parasites presenting short bulky flagella (Fig. 6D), immunogold labeling was carried out using the anti-FLA1 antibody raised against the extracellular domain (Nozaki et al., 1996) (Fig. 6E). Whereas no signal was detected in uninduced control cells, FLA1 was present at the cell surface of induced *IFT140^RNAi* parasites, following the path of the flagellum sleeve that itself is associated with the FAZ (Davidge et al., 2006).

Together, these data show that FLA1 is correctly targeted to the FAZ filament even in the absence of flagellum axoneme.

As FLAM3 is linked to the axoneme, its absence should not prevent FLA1 from being targeted to the FAZ filament. This was confirmed in *FLAM3^RNAi* cells where FLA1 was still present at the FAZ filament but was not encountered in the flagellum (Fig. 7A). Inversely, when expressed in *FLA1^RNAi* cells, FLAM3::YFP was observed in the cytoplasm and along the entire length of detached flagella (Fig. 7B), but not at the FAZ filament. Therefore, targeting of FLAM3 to the flagellum and its association with skeletal structures relies neither on the presence of FLA1 nor on flagellum attachment.

FLAM3 is required for proper distribution of FLA1BP

FLAM3 could function as a (direct or indirect) platform to anchor FLA1BP to the flagellar skeleton in a similar manner as the FAZ filament does for FLA1. To test this proposal, a YFP-tagged version of FLA1BP (Sun et al., 2012) was expressed in *FLAM3^RNAi* mutants. In the absence of tetracycline, FLA1BP was distributed at the flagellum membrane apparently along the FAZ, starting in the flagellar pocket from a region situated close to the starting point of the axoneme and ending in the region of the flagellum facing the anterior extremity of the cell body (Fig. 8A). The YFP::FLA1BP fluorescent signal was detergent resistant, showing a strong association to the flagellum skeleton (Fig. 8B). Strikingly, distribution of YFP::FLA1BP in the detached flagella of induced *FLAM3^RNAi* cells was restricted to the very proximal part of the flagellum, apparently corresponding to the short FAZ (Fig. 8C). FLA1BP::YFP was still present in detergent-extracted induced cells and appeared to be associated with the short FAZ root (Fig. 8D,E). In dividing cells, where only the new flagellum was detached, it presented a FLA1BP
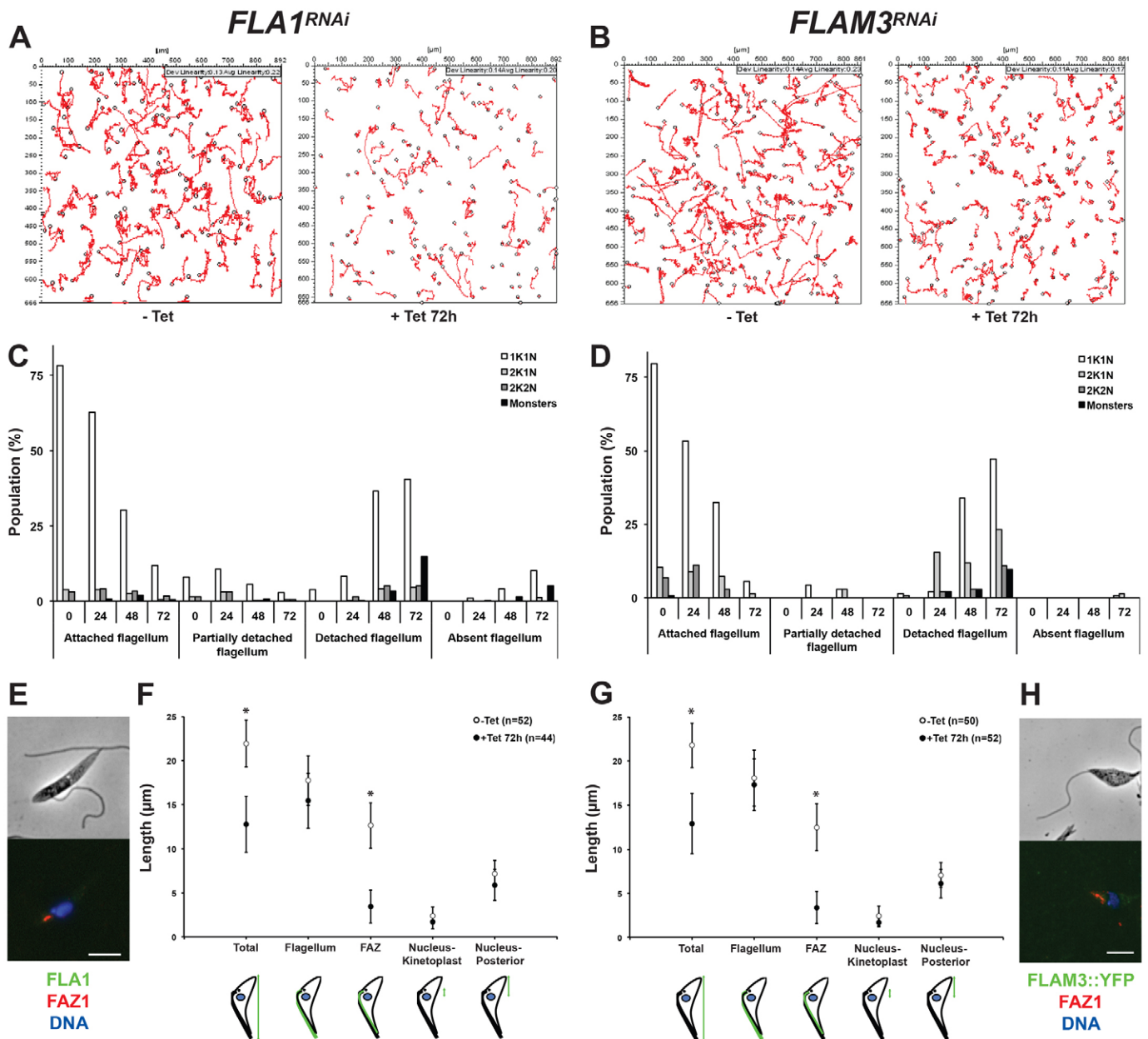
Fig. 4. Flagellum detachment upon depletion of FLA1 or FLAM3 impairs motility, cell division and cell morphogenesis. *In silico* tracking was performed on movies of *FLA1^RNAi* (A) and *FLAM3^RNAi* (B) cells. Representative sets of 2D tracks (200 cells for 20 seconds) of uninduced cells and cells induced for 72 hours are shown. *FLA1^RNAi* (C) and *FLAM3^RNAi* (D) cells were induced, fixed in methanol and stained with DAPI to analyze their phenotype according to (1) their DNA content [the number of kinetoplasts (K) and nuclei (N) is indicated as 1K1N, 2K1N, 2K2N and monsters for 1K0N or nKnN cells] and (2) the presence and level of attachment of their flagellum. Populations were plotted as the percentage of the total number of cells analyzed at each time point: *n*=285 at 0 hours, 289 at 24 hours, 268 at 48 hours and 176 at 72 hours for *FLA1^RNAi* mutants, and *n*=133 at 0 hours, 45 at 24 hours, 68 at 48 hours and 146 at 72 hours for *FLAM3^RNAi* mutants. (E,H) *FLA1^RNAi* (E) and *FLAM3^RNAi* (H) cells were induced for 72 hours, fixed in methanol and stained with DAPI (blue), the anti-FAZ1 antibody L3B2 (red), and the anti-FLA1 antibody Flap2 (green in E) or an anti-GFP antiserum (green in H). Scale bars: 5 µm. (F,G) *FLA1^RNAi* (F) and *FLAM3^RNAi* (G) cells were induced for 72 hours, fixed in methanol, stained with DAPI, the anti-FAZ1 L3B2 antibody and the mAb25 axoneme marker to allow morphological parameters measurements represented in the cartoons: total cell length, flagellum length, FAZ length, distance between the center of the nucleus and the kinetoplast, and distance between the center of the nucleus and the posterior end of 1K1N cells were plotted as lengths in µm ± s.d. Significant differences between uninduced (white) and cells induced for 72 hours (black) are indicated (*P<0.001).

labeling concentrated to its very proximal part. By contrast, the old flagellum displayed a normal FLA1BP distribution (Fig. 8E, arrows). This suggests that the FLA1–FLA1BP connection is first primed in the flagellar pocket, and then progressively established along the growing FAZ during the construction of the new flagellum.

DISCUSSION

The trypanosome flagellum is an essential organelle attached along the cell body where a highly specialized cytoskeletal structure called the FAZ filament has been proposed to mediate adhesion. This is supported by the knockdown of two components (FAZ1 and CC2D), which interferes with FAZ filament formation
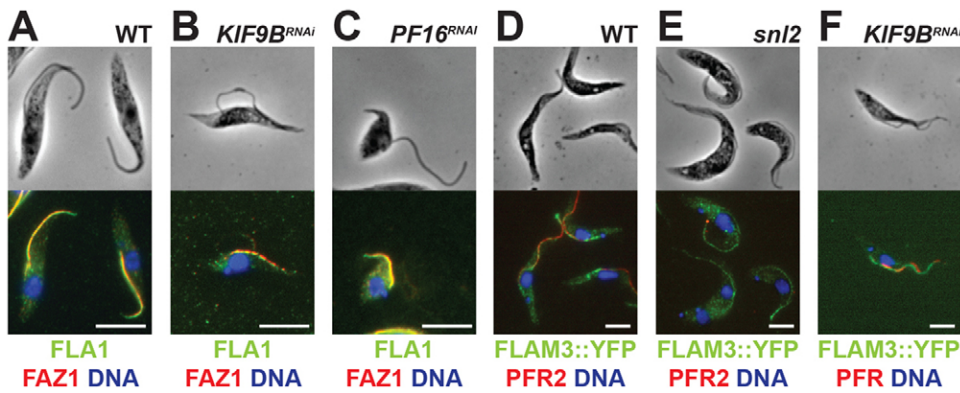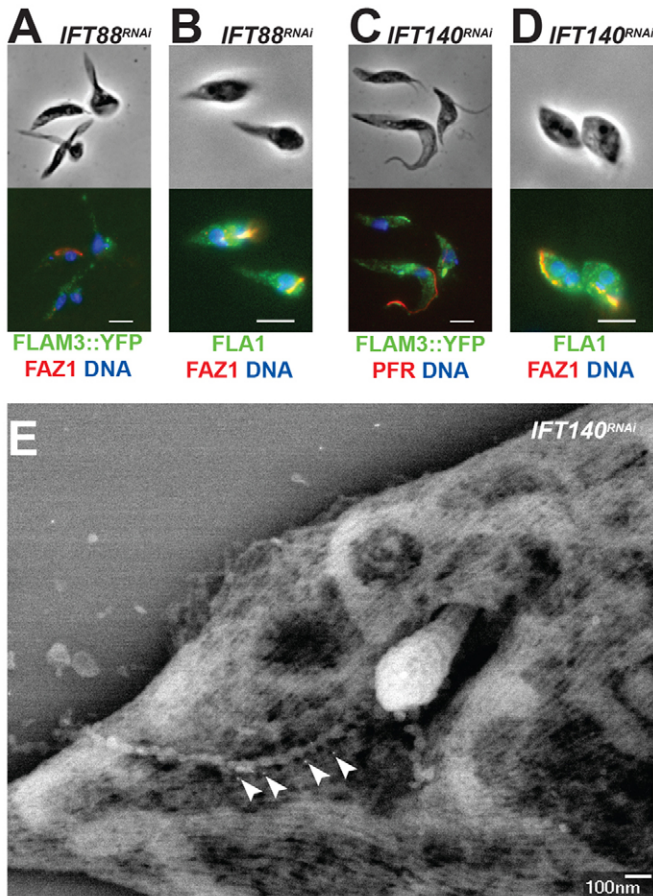
Fig. 5. FLAM3 is connected to the axoneme. WT (A,B), *snl-2* FLAM3::YFP (C), *KIF9B*^{RNAi} FLAM3::YFP (D), *KIF9B*^{RNAi} (E) and *PF16*^{RNAi} (F) cells were induced for 72 hours, fixed in methanol and stained with DAPI (blue), an anti-GFP antiserum (green in A,C,D) and the anti-PFR2 antibody L8C4 (red in A and C) or the anti-PFR1 and 2 L13D6 antibody (red in D), or the anti-FLA1 antibody Flap2 (green in B,E,F) and the anti-FAZ1 antibody L3B2 (red in B,E,F). Scale bars: 5 μm.
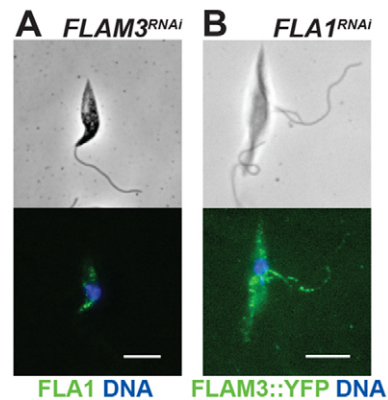
and results in flagellum detachment (Vaughan et al., 2008; Zhou et al., 2011). At least three other proteins are required for flagellar adhesion. One of them is specific to bloodstream form trypanosomes (Woods et al., 2013) and has not been investigated in this study focused on the procyclic stage. Two others, FLA1

Fig. 6. FLA1 is targeted to the FAZ through the flagellar pocket and is involved in the priming of the FAZ. *IFT88*^{RNAi} FLAM3::YFP (A), *IFT88*^{RNAi} (B), *IFT140*^{RNAi} FLAM3::YFP (C) and *IFT140*^{RNAi} (D) cells induced for 72 hours were stained with DAPI (blue), an anti-GFP antiserum (green in A and C) or the anti-FLA1 antibody Flap2 (green in B and D), and the anti-FAZ1 antibody L3B2 (red in A,B,D), or the anti-PFR2 antibody L8C4 (red in C). Scale bars: 5 μm. (E) *IFT140*^{RNAi} cells were induced for 72 hours and processed for scanning electron microscopy. Immunogold staining with the anti-FLA1 antibody in intact cells detects the protein (arrowheads) along a sleeve that follows the short FAZ. Scale bars: 100 nm.

(Cooper et al., 1993; LaCount et al., 2002) and FLA1BP (Sun et al., 2012), share a similar organization with a short intracellular domain, a transmembrane segment and a long extracellular region that contains NHL repeats (Sun et al., 2012). Here, we identified a novel protein termed FLAM3 that is also required for flagellum adhesion to the cell body. It does not contain any transmembrane domains but possesses a TPR motif, known for being prominent in flagellar proteins (Li et al., 2004), and it localizes to the flagellum.

We demonstrated that FLA1 is tightly linked to the FAZ filament on the cell body side where it colocalizes with FAZ1. This association takes place through its short intracellular C-terminus tail, whereas its N-terminal extracellular domain is not required but is responsible for the tight interaction with FLA1BP (Sun et al., 2012). FLA1BP would use its cytoplasmic tail to tether to the flagellum at the level of the FAZ connectors by the intermediate of FLAM3 (Fig. 9A). Three sets of interactions are therefore involved and these could be variably affected by different chemical treatments. This could explain why FLA1 appears linked to the flagellum skeleton upon extraction with Triton X-100 and to the FAZ filament on the cell body side upon treatment with Nonidet P-40. In the absence of FLA1, FLAM3 and FLA1BP target normally to the flagellum but adhesion fails to occur (Fig. 9B). However, localization of FLA1BP to the flagellum is severely modified in the absence of FLAM3: it is not properly distributed all along the organelle but restricted to a short proximal region, starting from the beginning of the axoneme
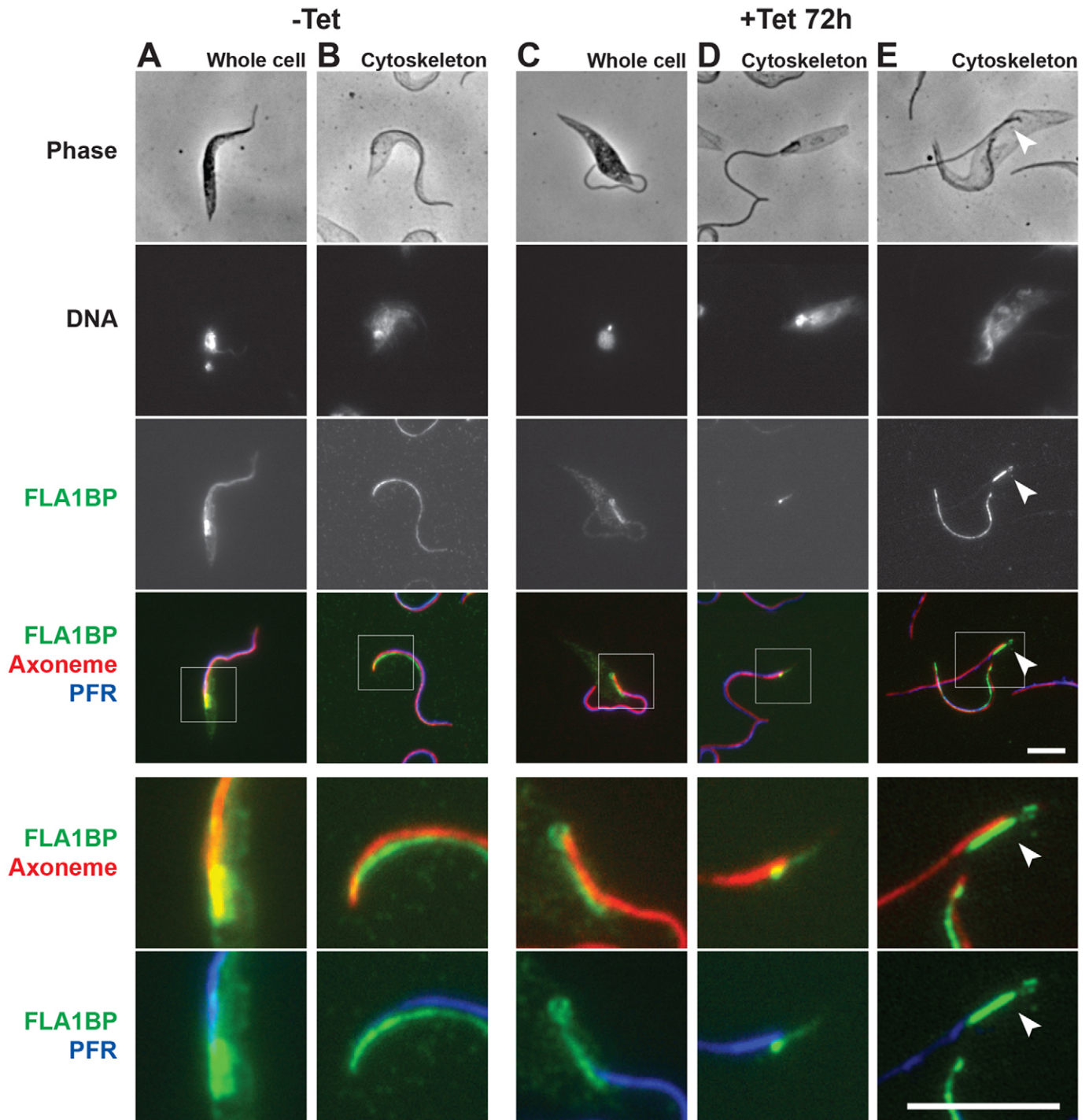

Fig. 7. FLA1 and FLAM3 are targeted to the FAZ independently. *FLAM3*^{RNAi} (A) and *FLA1*^{RNAi} FLAM3::YFP (B) cells induced for 72 hours were stained with DAPI (blue), the anti-FLA1 antibody Flap2 (green in A) or an anti-GFP antiserum (green in B). Scale bars: 5 μm.

Fig. 8. FLAM3 is necessary for the correct targeting of FLA1BP to the FAZ. (A–E) *FLAM3^RNAi* cells expressing YFP::FLA1BP were induced for 72 hours, directly fixed in methanol (A and C), or treated with NP40 (B,D,E), and stained with DAPI, an anti-GFP antiserum (green), the mAb25 axoneme marker (red) and the anti-PFR2 antibody L8C4 (blue). White boxes correspond to the areas enlarged in bottom panels. Scale bars: 5 μm. White arrowheads indicate the position of the new flagellum. In the absence of FLAM3, FLA1BP is restricted to the proximal portion of the flagellum.

and apparently parallel to the short FAZ (Fig. 9C). FLAM3 is therefore essential for proper FLA1BP distribution in the flagellum. This could be explained if FLA1BP was anchored to a skeletal element associated to the flagellum and if FLAM3 was either a component of, or a linker to this element. The PFR has been proposed to contribute to flagellum attachment (Demonchy et al., 2009; Ginger et al., 2013). However, perturbation of PFR

assembly upon ablation of PFR2 (albeit without visible alteration of the FAZ connectors) does not interfere with the regular distribution of FAZ1, FLA1, FLA1BP and FLAM3 (Fig. 9D).

In flagellum transverse sections, the FAZ connectors appear as a set of parallel fibers stretching from doublet 7 of the axoneme towards the area of adhesion. Although they are found in close proximity of the PFR, which is itself linked to the axoneme
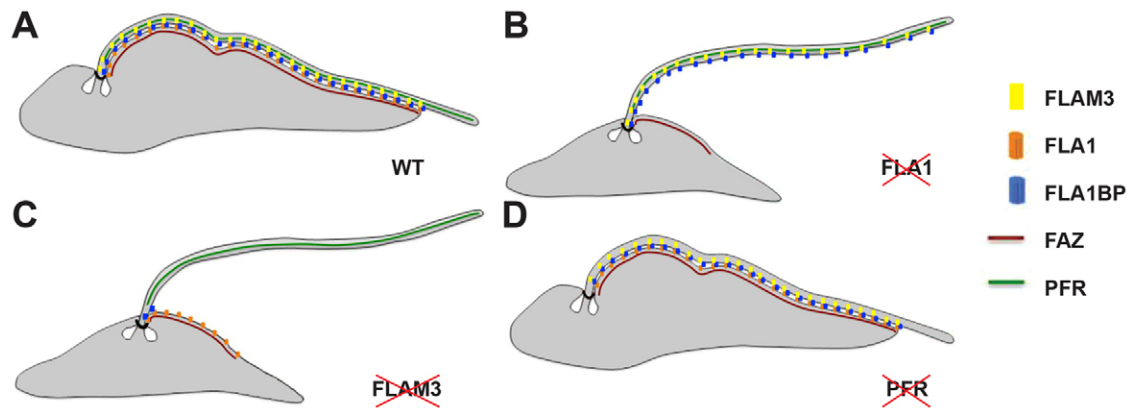
Fig. 9. An updated model of flagellum adhesion mediated by the molecular interactions of FLA1, FLA1-BP and FLAM3 with the cell body and the flagellum cytoskeleton structures. (A–D) Cartoons representing the relative positions and interactions of the main known FAZ components at the junction between the flagellum and the cell body [not drawn to scale, adapted from Sun et al. (Sun et al., 2012)]. Both FLA1 and FLAM3 are essential for flagellum adhesion along the cell body (WT in A): FLA1 is anchored to the FAZ filament in the cell body, and to its flagellum transmembrane partner FLA1BP outside; the latter is linked (directly or indirectly) to FLAM3, a new flagellum protein connected to the axoneme. FLAM3 and FLA1BP targeting to the flagellum are not dependent on the presence of FLA1 (B). However, in contrast to FLA1, which is present in the short FAZ filament, FLA1BP targeting relies on the presence of FLAM3 in the flagellum (C). The absence of PFR does not interfere with the interactions of FLA1, FLA1-BP and FLAM3, suggesting that FLAM3 is connected (directly or indirectly) to the axoneme.

between doublets 4 and 7, these fibers are present in the flagellar canal, a region of the flagellum situated in the flagellar pocket that lacks the PFR (Vickerman, 1969). The presence of these fibers has been confirmed by recent tomography studies (Gadelha et al., 2009; Lacomble et al., 2009). It should be noted that neither the FAZ filament nor the FAZ connectors appear to cross the cell body or the flagellum membrane (Vickerman, 1969; Bastin et al., 2000a). Several arguments support the view that FLAM3 is a component of the flagellar FAZ connectors. First, its distribution does not exactly follow the axoneme, as it is present in the flagellum at the vicinity of the cell body, almost from the base of the flagellum all along the axonemal marker Mab25 but finishing before the tip of the flagellum, close to the point where the adhesion with the cell body ends. Second, it is not directly associated with the core PFR structure, as revealed by its conserved localization in various PFR mutants (Fig. 9D). The FLAM3 signal is resistant to detergent extraction, which is expected for a skeletal element. Furthermore, FLAM3 could either be a structural component of the FAZ connectors, in agreement with the apparently reduced occurrence of these structures in the $FLAM3^{RNAi}$ mutant, or it could form a bridge from FLA1BP to the FAZ connectors without being essential for their construction. In both cases, depletion of FLAM3 is expected to disrupt FLA1BP distribution and hence the availability of FLA1BP to interact with FLA1, hence preventing flagellum attachment (Fig. 9C). Other proteins could be involved in the constitution of the FAZ connectors, such as the recently identified putative calcium channel FS179, which displays a distribution profile resembling that of FLAM3 and is also essential for flagellum attachment (Oberholzer et al., 2011).

This new model implies that the interaction between FLA1 and FLA1BP drives elongation of the FAZ during flagellum construction. These two proteins are probably synthesized in the endoplasmic reticulum and could interact together at the level of the flagellar pocket membrane, by binding their extracellular domains before connecting their intracellular ends to their respective skeleton structures. However, the normal targeting of each protein in the absence of the other suggests that the connection between them is established after they attach to

their respective structures and progresses while the flagellum elongates.

In addition to flagellum detachment, the second striking effect of RNAi silencing of *FLA1* and *FLAM3* is the inhibition of new FAZ elongation (Fig. 9B,C). Previous studies have suggested that the new flagellum and the new FAZ play important roles in flagellar pocket organization, basal body positioning and segregation (Kohl et al., 2003; Absalon et al., 2008b; Zhou et al., 2011). Whereas elongation of the new flagellum, with its distal end anchored to the old flagellum, pushes the new basal body away to the posterior end of the cell, the new FAZ might restrain the segregation and hold the new basal body in place. In cells depleted of BILBO-1, which is a component of the flagellar pocket collar, new FAZ assembly is completely inhibited and the new basal body is found at the far posterior end (Bonhivers et al., 2008). In $FLA1^{RNAi}$ and $FLAM3^{RNAi}$ cells, a short FAZ root was still present, possibly limiting the segregation of the new basal body from the old, such as in other mutants that lead to FAZ elongation defects (Absalon et al., 2007). The formation of this short FAZ root perhaps represents the initial FAZ nucleation, which occurs before and independently of new flagellum assembly (Kohl et al., 1999; Kohl et al., 2003). It has been shown previously that the FAZ length strongly correlates with the cell size and morphology in culture (Kohl et al., 2003; Zhou et al., 2011) and during parasite development (Rotureau et al., 2011). This is best explained if the position of the FAZ defines the axis of cytokinesis (Robinson et al., 1995). Therefore, the reduced length of the FAZ root observed in $FLA1^{RNAi}$ (3.4±1.9 µm) and $FLAM3^{RNAi}$ (3.4±1.8 µm) cells compared with that measured in $FLA1BP^{RNAi}$ (5.8±1.6 µm) (Sun et al., 2012) could explain the incapacity of these mutants to proliferate. It could be proposed that the short FAZ of $FLA1BP^{RNAi}$ cells that yet reaches the anterior extremity of the cell body is sufficiently elongated to properly act as an ingression furrow during cytokinesis. By contrast, cytokinesis is not achieved in $FLA1^{RNAi}$ and $FLAM3^{RNAi}$ cells where the FAZ root ends in the middle of the cell body length.

In summary, we propose a new detailed molecular model for the structural organization of the FAZ in trypanosomes that

integrates the FAZ connectors and a novel flagellum component. Further studies are now required to unravel the full molecular nature of the FAZ connectors, the processes of assembly of the FAZ and the way it governs cell morphogenesis, especially *in vivo*.

MATERIALS AND METHODS

Trypanosome cell lines and cultures

All cell lines were derivatives of strain 427 of *T. brucei* and cultured in SDM79 medium supplemented with hemin and 10% fetal calf serum. Cell lines *FLA1^{RNAi}* (LaCount et al., 2002), *IFT88^{RNAi}* (Kohl et al., 2003), *IFT140^{RNAi}* (Absalon et al., 2008a), *KIF9B^{RNAi}* (Demonchy et al., 2009), *snl-2* (Bastin et al., 2000a) and *PF16^{RNAi}* (Branche et al., 2006) have previously been described and all express double-stranded RNA from tetracycline-inducible T7 promoters (Wirtz et al., 1999). For the construction of the FLAM3::YFP cell lines, the last 572 bp of *FLAM3* coding sequence (Tb927.8.4780) without the stop codon (11,881–12,453 bp) was synthesized (GeneCust Europe, Luxembourg) and cloned with *Sph*I and *Bam*HI into the p3329 vector (Kelly et al., 2007) to be integrated in one copy of the gene for endogenous expression. For the construction of the inducible *FLAM3^{RNAi}* cell line, a 373 bp target fragment of the gene (3961–4333 bp) was synthesized (Genecust Europe, Luxembourg) and cloned with *Xho*I and *Hin*dIII in the pZJM vector (Wang et al., 2000) for transformation of the 29.13 cell line (Wirtz et al., 1999). The pHD1034-FLA1BP plasmid was used for constitutive overexpression of YFP::FLA1BP (Sun et al., 2012). All vectors were separately nucleofected (Lonza) in various cell lines and antibiotic-resistant cells with the highest YFP signal or the clearest distinction between non-induced and induced samples were selected for subcloning by limiting dilution. Induction of RNAi cell lines was achieved by the addition of 1 µg tetracycline per ml of medium and fresh tetracycline was added at each cell dilution. Cell culture growth was monitored daily with a Z2 cell counter (Beckman Coulter).

Immunofluorescence analysis and morphogenetic measurements

Intact cells were treated for immunofluorescence after paraformaldehyde (PFA) or methanol fixation as described previously (Rotureau et al., 2011; Rotureau et al., 2012). Cytoskeletons were detergent-extracted with 1% Triton X-100 or 1% Nonidet-P40 in PEM buffer (100 mM PIPES, pH 6.9, 1 mM EGTA, 1 mM $MgSO_4$) for 10 minutes, washed in PBS and fixed in methanol as described elsewhere (Sherwin et al., 1987; Sherwin and Gull, 1989a). MAb25 (IgG2a) labels a protein found all along the axoneme (Pradel et al., 2006). As PFR markers, we used the monoclonal antibodies L8C4 (IgG1), which specifically recognizes PFR2, and L13D6 (IgG1) for both PFR1 and PFR2 (Kohl et al., 1999). L3B2 (IgG1) targets the FAZ1 protein (Kohl et al., 1999; Vaughan et al., 2008), whereas DOT-1 (IgM, 1:2) labels a different component of the FAZ filament (Woods et al., 1989). FLA1 was labeled with the rat antibody Flap2 (1:50) (Nozaki et al., 1996). The YFP tag was detected with a rabbit anti-GFP antibody (Invitrogen). Subclass-specific secondary antibodies coupled to FITC (Sigma), Alexa Fluor 488 (Invitrogen), Cy3 or Cy5 (Jackson) were used for double labeling. Slides were stained with 4′,6-diamidino-2-phenylindole (DAPI) for visualization of kinetoplast and nuclear DNA content and mounted in Prolong (Invitrogen) for microscopic observations. For each antibody, immunofluorescence analysis was repeated at least in three distinct experiments.

Samples were observed either with a DMR microscope (Leica), when images were captured with a CoolSnap HQ camera (Roper Scientific), or with a DMI4000 microscope (Leica), when images were acquired with a Retiga-SRV camera (Q-Imaging). Pictures were analyzed and cell parameters were measured using the IPLab Spectrum 3.9 software (Scanalytics & BD Biosciences) or the ImageJ 1.47e software (NIH). For clarity purposes, brightness and contrast of several pictures were adjusted after their analysis in accordance with editorial policies. The scale bars represent 5 µm in most immunofluorescence figures, except when indicated otherwise. Flagellum length was measured using L8C4 and

L13D6 PFR markers and FAZ length using L3B2 and DOT-1 labeling. Morphometric measurements (µm) and cell counts were done as previously described (Rotureau et al., 2011; Rotureau et al., 2012) and plotted as mean ± s.d. Statistical analyses were performed in Excel or with the KaleidaGraph V.4.0 software (Synergy Software). Two-tailed unpaired *t*-tests were performed and significant results were indicated with *$P < 0.0001$.

Motility analyses

For each time of induction (0, 24 hours, 48 hours and 72 hours), movies were recorded (200 frames, 50 ms of exposure). Samples were observed in warm medium at 5×10^6 cells/ml under the 10× objective of an inverted DMI4000 LEICA microscope (Leica) coupled to a Retiga-SRV camera (QImaging). Movies were converted with the MPEG Streamclip V.1.9b3 software (Squared 5) and analyzed with the medeaLAB CASA Tracking V.5.5 software (medea AV GmbH). For each movie, up to 199 cells were simultaneously tracked *in silico*.

Electron microscopy

Cell fixation, embedding and sectioning for transmission electron microscopy of whole cells from wild-type and induced *FLA1^{RNAi}* and *FLAM3^{RNAi}* samples was carried out as described previously (Branche et al., 2006). For scanning electron microscopy of whole cells, samples were prepared and analyzed as described previously (Absalon et al., 2007). For immunogold detection with L3B2, DOT-1, Flap2 and anti-GFP, cells were treated as described previously (Absalon et al., 2008b), except that bound antibodies were detected by the addition of subclass specific secondary antibodies conjugated to gold particles of 10, 20, 30 or 40 nm diameter (BB International) in PBS with 1% BSA. For cytoskeleton observations, cells were treated with 1% Triton X-100 or 1% Nonidet P-40 at 4°C in PBS for 10 minutes to strip the plasma membrane. Samples were washed twice in PBS, fixed in glutaraldehyde and processed for scanning electron microscopy in standard conditions (Absalon et al., 2007; Absalon et al., 2008b).

RT-PCR

Total RNA was extracted from wild-type and *FLAM3^{RNAi}* cells grown with or without tetracycline for the indicated periods of time and purified using TRIzol (Invitrogen). DNA was eliminated by DNase treatment (Qiagen) and RNA purity was confirmed by conventional PCR. After primer calibration and determination of optimal conditions, semi-quantitative RT-PCR was performed according to the manufacturer recommendations with a SuperScript One-step RT-PCR Platinum-Taq kit (Invitrogen). Primers were selected to hybridize outside the region selected for dsRNA expression to avoid amplification of RNA deriving from the dsRNA trigger. Primers CTTCAGAGGGCATCTAGAAAG (11,875–11,895 in the coding sequence) and CCTTGAAGATTCAGCAGGCGC (12,424–12,444) targeting a 570 bp sequence were used for FLAM3, and primers amplifying a 697 bp region of the *ODA7* gene (Duquesnoy et al., 2009) were selected as control primers.

Supplementary material

Supplementary material available online at
http://jcs.biologists.org/lookup/suppl/doi:10.1242/jcs.136424/-/DC1

References

Absalon, S., Kohl, L., Branche, C., Blisnick, T., Toutirais, G., Rusconi, F., Cosson, J., Bonhivers, M., Robinson, D. and Bastin, P. (2007). Basal body positioning is controlled by flagellum formation in Trypanosoma brucei. *PLoS ONE* **2**, e437.

Absalon, S., Blisnick, T., Kohl, L., Toutirais, G., Doré, G., Julkowska, D., Tavenet, A. and Bastin, P. (2008a). Intraflagellar transport and functional analysis of genes required for flagellum formation in trypanosomes. *Mol. Biol. Cell* **19**, 929-944.

Absalon, S., Blisnick, T., Bonhivers, M., Kohl, L., Cayet, N., Toutirais, G., Buisson, J., Robinson, D. and Bastin, P. (2008b). Flagellum elongation is required for correct structure, orientation and function of the flagellar pocket in Trypanosoma brucei. *J. Cell Sci.* **121**, 3704-3716.

Adhiambo, C., Blisnick, T., Toutirais, G., Delannoy, E. and Bastin, P. (2009). A novel function for the atypical small G protein Rab-like 5 in the assembly of the trypanosome flagellum. *J. Cell Sci.* **122**, 834-841.

Bastin, P., Sherwin, T. and Gull, K. (1998). Paraflagellar rod is vital for trypanosome motility. *Nature* **391**, 548.

Bastin, P., Ellis, K., Kohl, L. and Gull, K. (2000a). Flagellum ontogeny in trypanosomes studied via an inherited and regulated RNA interference system. *J. Cell Sci.* **113**, 3321-3328.

Bastin, P., Pullen, T. J., Moreira-Leite, F. F. and Gull, K. (2000b). Inside and outside of the trypanosome flagellum:a multifunctional organelle. *Microbes Infect.* **2**, 1865-1874.

Bonhivers, M., Nowacki, S., Landrein, N. and Robinson, D. R. (2008). Biogenesis of the trypanosome endo-exocytotic organelle is cytoskeleton mediated. *PLoS Biol.* **6**, e105.

Branche, C., Kohl, L., Toutirais, G., Buisson, J., Cosson, J. and Bastin, P. (2006). Conserved and specific functions of axoneme components in trypanosome motility. *J. Cell Sci.* **119**, 3443-3455.

Broadhead, R., Dawe, H. R., Farr, H., Griffiths, S., Hart, S. R., Portman, N., Shaw, M. K., Ginger, M. L., Gaskell, S. J., McKean, P. G. et al. (2006). Flagellar motility is required for the viability of the bloodstream trypanosome. *Nature* **440**, 224-227.

Brun, R., Blum, J., Chappuis, F. and Burri, C. (2010). Human African trypanosomiasis. *Lancet* **375**, 148-159.

Cooper, R., Inverso, J. A., Espinosa, M., Nogueira, N. and Cross, G. A. (1991). Characterization of a candidate gene for GP72, an insect stage-specific antigen of Trypanosoma cruzi. *Mol. Biochem. Parasitol.* **49**, 45-59.

Cooper, R., de Jesus, A. R. and Cross, G. A. (1993). Deletion of an immunodominant Trypanosoma cruzi surface glycoprotein disrupts flagellum-cell adhesion. *J. Cell Biol.* **122**, 149-156.

Davidge, J. A., Chambers, E., Dickinson, H. A., Towers, K., Ginger, M. L., McKean, P. G. and Gull, K. (2006). Trypanosome IFT mutants provide insight into the motor location for mobility of the flagella connector and flagellar membrane formation. *J. Cell Sci.* **119**, 3935-3943.

Demonchy, R., Blisnick, T., Deprez, C., Toutirais, G., Loussert, C., Marande, W., Grellier, P., Bastin, P. and Kohl, L. (2009). Kinesin 9 family members perform separate functions in the trypanosome flagellum. *J. Cell Biol.* **187**, 615-622.

Duquesnoy, P., Escudier, E., Vincensini, L., Freshour, J., Bridoux, A. M., Coste, A., Deschildre, A., de Blic, J., Legendre, M., Montantin, G. et al. (2009). Loss-of-function mutations in the human ortholog of Chlamydomonas reinhardtii ODA7 disrupt dynein arm assembly and cause primary ciliary dyskinesia. *Am. J. Hum. Genet.* **85**, 890-896.

Emmer, B. T., Daniels, M. D., Taylor, J. M., Epting, C. L. and Engman, D. M. (2010). Calflagin inhibition prolongs host survival and suppresses parasitemia in Trypanosoma brucei infection. *Eukaryot. Cell* **9**, 934-942.

Engstler, M., Pfohl, T., Herminghaus, S., Boshart, M., Wiegertjes, G., Heddergott, N. and Overath, P. (2007). Hydrodynamic flow-mediated protein sorting on the cell surface of trypanosomes. *Cell* **131**, 505-515.

Gadelha, C., Rothery, S., Morphew, M., McIntosh, J. R., Severs, N. J. and Gull, K. (2009). Membrane domains and flagellar pocket boundaries are influenced by the cytoskeleton in African trypanosomes. *Proc. Natl. Acad. Sci. USA* **106**, 17425-17430.

Ginger, M. L., Collingridge, P. W., Brown, R. W., Sproat, R., Shaw, M. K. and Gull, K. (2013). Calmodulin is required for paraflagellar rod assembly and flagellum-cell body attachment in trypanosomes. *Protist* **164**, 528-540.

Griffiths, S., Portman, N., Taylor, P. R., Gordon, S., Ginger, M. L. and Gull, K. (2007). RNA interference mutant induction in vivo demonstrates the essential nature of trypanosome flagellar function during mammalian infection. *Eukaryot. Cell* **6**, 1248-1250.

Haynes, P. A., Russell, D. G. and Cross, G. A. (1996). Subcellular localization of Trypanosoma cruzi glycoprotein Gp72. *J. Cell Sci.* **109**, 2979-2988.

Kelly, S., Reed, J., Kramer, S., Ellis, L., Webb, H., Sunter, J., Salje, J., Marinsek, N., Gull, K., Wickstead, B. et al. (2007). Functional genomics in Trypanosoma brucei: a collection of vectors for the expression of tagged proteins from endogenous and ectopic gene loci. *Mol. Biochem. Parasitol.* **154**, 103-109.

Kohl, L. and Gull, K. (1998). Molecular architecture of the trypanosome cytoskeleton. *Mol. Biochem. Parasitol.* **93**, 1-9.

Kohl, L., Sherwin, T. and Gull, K. (1999). Assembly of the paraflagellar rod and the flagellum attachment zone complex during the Trypanosoma brucei cell cycle. *J. Eukaryot. Microbiol.* **46**, 105-109.

Kohl, L., Robinson, D. and Bastin, P. (2003). Novel roles for the flagellum in cell morphogenesis and cytokinesis of trypanosomes. *EMBO J.* **22**, 5336-5346.

Lacomble, S., Vaughan, S., Gadelha, C., Morphew, M. K., Shaw, M. K., McIntosh, J. R. and Gull, K. (2009). Three-dimensional cellular architecture of the flagellar pocket and associated cytoskeleton in trypanosomes revealed by electron microscope tomography. *J. Cell Sci.* **122**, 1081-1090.

LaCount, D. J., Barrett, B. and Donelson, J. E. (2002). Trypanosoma brucei FLA1 is required for flagellum attachment and cytokinesis. *J. Biol. Chem.* **277**, 17580-17588.

Li, J. B., Gerdes, J. M., Haycraft, C. J., Fan, Y., Teslovich, T. M., May-Simera, H., Li, H., Blacque, O. E., Li, L., Leitch, C. C. et al. (2004). Comparative genomics identifies a flagellar and basal body proteome that includes the BBS5 human disease gene. *Cell* **117**, 541-552.

Moreira-Leite, F. F., Sherwin, T., Kohl, L. and Gull, K. (2001). A trypanosome structure involved in transmitting cytoplasmic information during cell division. *Science* **294**, 610-612.

Nozaki, T., Haynes, P. A. and Cross, G. A. (1996). Characterization of the Trypanosoma brucei homologue of a Trypanosoma cruzi flagellum-adhesion glycoprotein. *Mol. Biochem. Parasitol.* **82**, 245-255.

Oberholzer, M., Langousis, G., Nguyen, H. T., Saada, E. A., Shimogawa, M. M., Jonsson, Z. O., Nguyen, S. M., Wohlschlegel, J. A. and Hill, K. L. (2011). Independent analysis of the flagellum surface and matrix proteomes provides insight into flagellum signaling in mammalian-infectious Trypanosoma brucei. *Mol. Cell. Proteomics* **10**, M111 010538.

Pradel, L. C., Bonhivers, M., Landrein, N. and Robinson, D. R. (2006). NIMA-related kinase TbNRKC is involved in basal body separation in Trypanosoma brucei. *J. Cell Sci.* **119**, 1852-1863.

Ralston, K. S., Lerner, A. G., Diener, D. R. and Hill, K. L. (2006). Flagellar motility contributes to cytokinesis in Trypanosoma brucei and is modulated by an evolutionarily conserved dynein regulatory system. *Eukaryot. Cell* **5**, 696-711.

Ralston, K. S., Kabututu, Z. P., Melehani, J. H., Oberholzer, M. and Hill, K. L. (2009). The Trypanosoma brucei flagellum: moving parasites in new directions. *Annu. Rev. Microbiol.* **63**, 335-362.

Robinson, D. R. and Gull, K. (1991). Basal body movements as a mechanism for mitochondrial genome segregation in the trypanosome cell cycle. *Nature* **352**, 731-733.

Robinson, D. R., Sherwin, T., Ploubidou, A., Byard, E. H. and Gull, K. (1995). Microtubule polarity and dynamics in the control of organelle positioning, segregation, and cytokinesis in the trypanosome cell cycle. *J. Cell Biol.* **128**, 1163-1172.

Rocha, G. M., Brandão, B. A., Mortara, R. A., Attias, M., de Souza, W. and Carvalho, T. M. (2006). The flagellar attachment zone of Trypanosoma cruzi epimastigote forms. *J. Struct. Biol.* **154**, 89-99.

Rocha, G. M., Seabra, S. H., de Miranda, K. R., Cunha-e-Silva, N., de Carvalho, T. M. and de Souza, W. (2010). Attachment of flagellum to the cell body is important to the kinetics of transferrin uptake by Trypanosoma cruzi. *Parasitol. Int.* **59**, 629-633.

Rodríguez, J. A., Lopez, M. A., Thayer, M. C., Zhao, Y., Oberholzer, M., Chang, D. D., Kisalu, N. K., Penichet, M. L., Helguera, G., Bruinsma, R. et al. (2009). Propulsion of African trypanosomes is driven by bihelical waves with alternating chirality separated by kinks. *Proc. Natl. Acad. Sci. USA* **106**, 19322-19327.

Rotureau, B., Subota, I. and Bastin, P. (2011). Molecular bases of cytoskeleton plasticity during the Trypanosoma brucei parasite cycle. *Cell. Microbiol.* **13**, 705-716.

Rotureau, B., Subota, I., Buisson, J. and Bastin, P. (2012). A new asymmetric division contributes to the continuous production of infective trypanosomes in the tsetse fly. *Development* **139**, 1842-1850.

Sharma, R., Gluenz, E., Peacock, L., Gibson, W., Gull, K. and Carrington, M. (2009). The heart of darkness: growth and form of Trypanosoma brucei in the tsetse fly. *Trends Parasitol.* **25**, 517-524.

Sherwin, T. and Gull, K. (1989a). The cell division cycle of Trypanosoma brucei brucei: timing of event markers and cytoskeletal modulations. *Philos. Trans. R. Soc. B* **323**, 573-588.

Sherwin, T. and Gull, K. (1989b). Visualization of detyrosination along single microtubules reveals novel mechanisms of assembly during cytoskeletal duplication in trypanosomes. *Cell* **57**, 211-221.

Sherwin, T., Schneider, A., Sasse, R., Seebeck, T. and Gull, K. (1987). Distinct localization and cell cycle dependence of COOH terminally tyrosinolated alpha-tubulin in the microtubules of Trypanosoma brucei brucei. *J. Cell Biol.* **104**, 439-446.

Sun, Y., Wang, C., Yuan, Y. A. and He, C. Y. (2012). An intracellular membrane junction mediated by flagellum adhesion glycoproteins links flagellum biogenesis to cell morphogenesis in Trypanosoma brucei. *J. Cell Sci.* **126**, 520-531.

Tetley, L. and Vickerman, K. (1985). Differentiation in Trypanosoma brucei: host-parasite cell junctions and their persistence during acquisition of the variable antigen coat. *J. Cell Sci.* **74**, 1-19.

Vaughan, S. (2010). Assembly of the flagellum and its role in cell morphogenesis in Trypanosoma brucei. *Curr. Opin. Microbiol.* **13**, 453-458.

Vaughan, S., Kohl, L., Ngai, I., Wheeler, R. J. and Gull, K. (2008). A repetitive protein essential for the flagellum attachment zone filament structure and function in Trypanosoma brucei. *Protist* **159**, 127-136.

Vickerman, K. (1969). On the surface coat and flagellar adhesion in trypanosomes. *J. Cell Sci.* **5**, 163-193.

Wang, Z., Morris, J. C., Drew, M. E. and Englund, P. T. (2000). Inhibition of Trypanosoma brucei gene expression by RNA interference using an integratable vector with opposing T7 promoters. *J. Biol. Chem.* **275**, 40174-40179.

Weiße, S., Heddergott, N., Heydt, M., Pflästerer, D., Maier, T., Haraszti, T., Grunze, M., Engstler, M. and Rosenhahn, A. (2012). A quantitative 3D motility analysis of Trypanosoma brucei by use of digital in-line holographic microscopy. *PLoS ONE* **7**, e37296.

Wirtz, E., Leal, S., Ochatt, C. and Cross, G. A. (1999). A tightly regulated inducible expression system for conditional gene knock-outs and dominant-negative genetics in Trypanosoma brucei. *Mol. Biochem. Parasitol.* **99**, 89-101.

Woods, A., Sherwin, T., Sasse, R., MacRae, T. H., Baines, A. J. and Gull, K. (1989). Definition of individual components within the cytoskeleton of Trypanosoma brucei by a library of monoclonal antibodies. *J. Cell Sci.* **93**, 491-500.

Woods, K., Nic a'Bhaird, N., Dooley, C., Perez-Morga, D. and Nolan, D. P. (2013). Identification and characterization of a stage specific membrane protein involved in flagellar attachment in Trypanosoma brucei. *PLoS ONE* **8**, e52846.

Zhou, Q., Gheiratmand, L., Chen, Y., Lim, T. K., Zhang, J., Li, S., Xia, N., Liu, B., Lin, Q. and He, C. Y. (2010). A comparative proteomic analysis reveals a new bi-lobe protein required for bi-lobe duplication and cell division in Trypanosoma brucei. *PLoS ONE* **5**, e9660.

Zhou, Q., Liu, B., Sun, Y. and He, C. Y. (2011). A coiled-coil- and C2-domain-containing protein is required for FAZ assembly and cell morphology in Trypanosoma brucei. *J. Cell Sci.* **124**, 3848-3858.
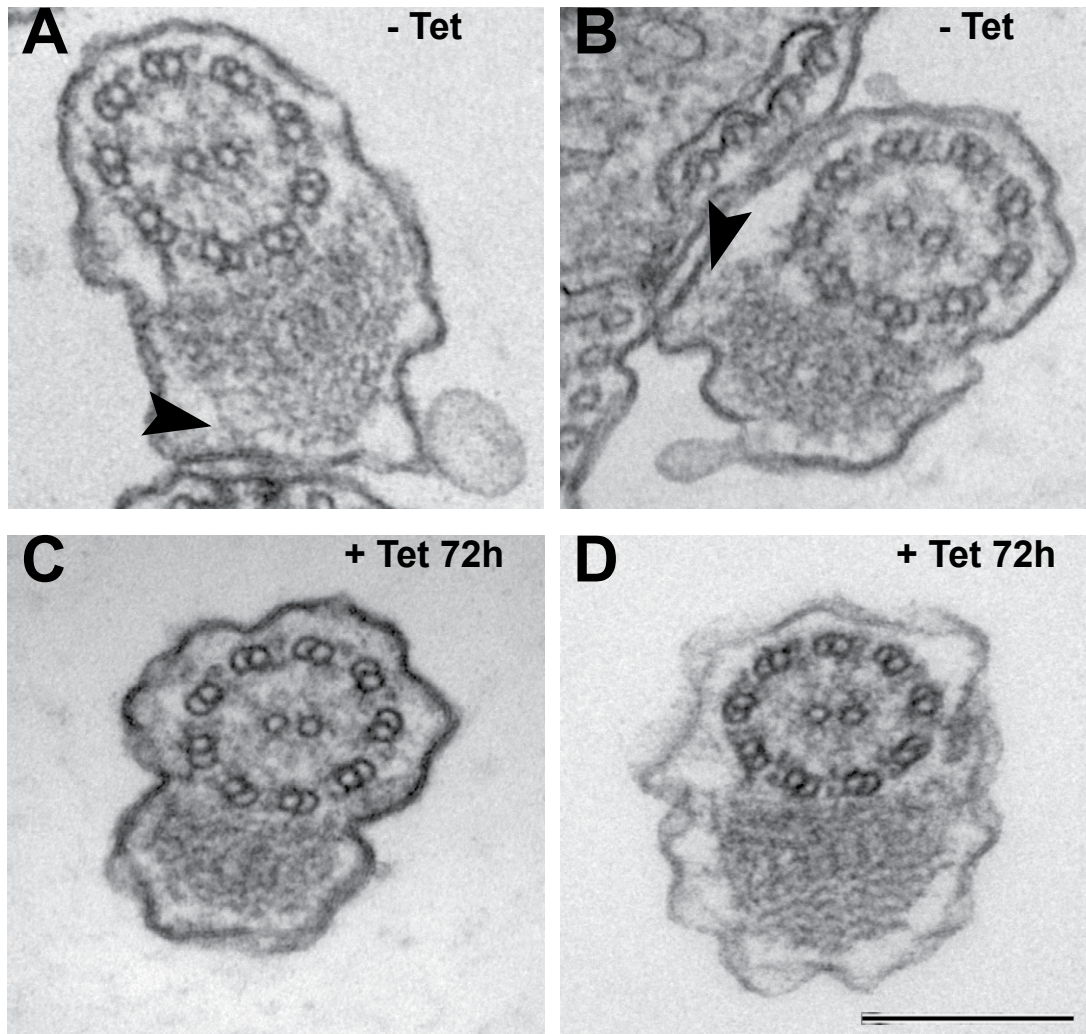
Fig. S1. FLAM3 is part of the flagellum connectors. Sections through the flagellum of *FLAM3^RNAi* cells uninduced (A,B) or induced for 72 hours (C,D) analyzed by transmission electron microscopy. Black arrowheads show the FAZ connectors, fibers apparently connecting the axoneme to the FAZ region.